ELSEVIER

Journal of Chromatography A, 877 (2000) 41–59

JOURNAL OF CHROMATOGRAPHY A

www.elsevier.com/locate/chroma

Characterization of C_{18}-bonded liquid chromatographic stationary phases by Raman spectroscopy: the effect of temperature

Charles A. Doyle[a], Thomas J. Vickers[b], Charles K. Mann[b], John G. Dorsey[b,*]

[a]*Department of Chemistry, University of Cincinnati, Cincinnati, OH 45221-0172, USA*

[b]*Department of Chemistry, Florida State University, Tallahassee, FL 32306-4390, USA*

Received 2 June 1998; received in revised form 25 November 1999; accepted 29 December 1999

Abstract

This study represents the first time that both the mobile phase composition and the temperature are simultaneously controlled to examine silica-bonded octadecylsilyl (C_{18}) ligands spectroscopically at typical liquid chromatographic (LC) mobile phase flow-rates and back-pressures. Raman spectroscopy is used to characterize the behavior of the C_{18} bonded ligands equilibrated at temperatures from 45 to 2°C in neat, single-component, mobile phase solvents including: water, acetonitrile, methanol, and chloroform. In addition, the effect of stationary phase ligand bonding density is examined by using two different monomeric reversed-phase liquid chromatographic (RPLC) stationary phases, a 2.34 and a 3.52 μmol m^{-2} Microporasil C_{18} stationary phase, under identical conditions. The direct, on-column, spectroscopic analysis used in this study allows direct evaluation of the temperature-dependent behavior of the bonded C_{18} ligands. The temperature-dependent ordering of the stationary phase ligands is examined to determine if the ligands undergo a phase transition from a less-ordered ''liquid-like'' state at higher temperatures to a more-ordered ''solid-like'' state at lower temperatures. A discrete phase transition was not observed, but rather a continual ordering as temperature was lowered.

Keywords: Stationary phases, LC; Raman spectroscopy; Temperature effects; Mobile phase composition

1. Introduction

Temperature, or thermal, equilibration is a relatively under-utilized parameter in liquid chromatographic separations. First, it is essential to control the temperature of the LC system to obtain reproducible measurements. Retention times can vary appreciably with even slight fluctuations in operating temperature. In addition, selectivity can be optimized at subambient temperatures [1–3]; whereas higher temperatures improve the speed of analysis, which is particularly advantageous in the analyses of peptides and proteins [4]. Recently, Zhu et al. [5–8] have examined the use of temperature as an additional parameter in semi-empirical relationships for the prediction of separation in reversed-phase gradient elution chromatography. Also, temperature is an additional parameter which can be exploited to examine the thermodynamics of retention.

Temperature studies have typically been performed to examine the thermodynamic driving forces and the mechanisms of solute retention in RPLC.

*Corresponding author.

0021-9673/00/$ – see front matter
PII: S0021-9673(00)00174-6

The van't Hoff relationship ($\ln k'$ versus $1/T$) has been used to examine RPLC retention behavior and to obtain thermodynamic information. Plots of the natural logarithm of the solute capacity factor ($\ln k'$) as a function of the inverse of temperature in Kelvin ($1/T$) often yields a linear relationship [1,2,9–18] from which enthalpy ($\Delta H°$) and entropy ($\Delta S°$) values can be obtained using the following expression:

$$\ln k' = \frac{-\Delta H°}{RT} + \frac{\Delta S°}{R} + \ln \phi$$

where R is the ideal gas constant, ϕ is the volume phase ratio ($\phi = V_s/V_m$), or the ratio of stationary phase (V_s) to mobile phase (V_m) volumes, and $\Delta H°$ and $\Delta S°$ are the enthalpy and entropy of solute transfer from the mobile phase to the stationary phase, respectively. From a mechanistic standpoint, achievement of linear van't Hoff relationships is interpreted to indicate that the same retention mechanism is operative over the temperature range investigated.

Non-linear van't Hoff relationships have also been obtained for chemically-bonded silica-based liquid chromatographic stationary phases, and related materials, using both liquid [1,2,10,11,13,17–22] and gaseous [23–28] mobile phases. These non-linear van't Hoff relationships often consist of two linear regions, of differing slopes, which either intersect at a particular temperature or are joined by a sigmoidal region over a narrow temperature range (referred to as the ''onset temperature''). Deviations from linearity have usually been interpreted as indicating that either the retention mechanism and/or the stationary phase structure has varied within the temperature range examined. One possible explanation for the observed deviations from linearity has been that the stationary phase ligands undergo a ''phase transition'' from a less ordered ''liquid-like'' state at temperatures above this onset temperature (or phase transition temperature) to a more ordered ''solid-like'' state below this transition temperature.

The onset temperatures of these phase transitions observed by van't Hoff analyses have been found to depend upon the stationary phase ligand chain length, bonding density, and functionality (monomeric versus polymeric); the composition of the mobile phase; and the types of solutes examined. In support of the occurrence of bonded ligand phase transitions, the onset temperature for high bonding density monomeric C_{18} stationary phases ligands has typically been observed near 25–30°C, which corresponds to the phase transition temperature (28–30°C) of neat octadecane.

The deviations from linearity observed by gas chromatography [20,23,24,27,28] have been attributed to a reversible ''fusion-like'' phase transition [23] of the bonded chains, from ''a type of crystallized state'' in which the bonded chains are tilted toward the support surface below the phase transition temperature to a ''liquid expanded state'' at higher temperatures. Liquid chromatographic results [20] were also attributed to a similar phase transition behavior of the stationary phase ligands. In the liquid chromatographic studies [20], the transition temperature was observed to depend on the composition of the mobile phase. The retention process in the liquid chromatographic studies [20] was further attributed to a transition from an adsorption-dominant mechanism at the surface of the ''solid'' monolayer to a solution-dominant mechanism in the ''liquid expanded-like layer''.

Gilpin and coworkers [10,19,29] observed another type of temperature-dependent phase transition in which the stationary phase ligands in a neat water mobile phase have been found to undergo an irreversible thermal reorganization with increasing temperature so as to release residual organic solvent that had been trapped by the ligands at the lower temperatures during organic solvent pre-treatments.

Wheeler et al. [30] have reviewed the evidence in support of the occurrence of phase transitions for bonded reversed-phase liquid chromatographic ligands, and the effects these phase transitions have on retention mechanisms. More direct evidence for the occurrence of phase transitions has come from contact angle measurements [31], specific heat measurements using adiabatic calorimetry [32], differential scanning calorimetry [13,17,27,28,33,34], infrared spectroscopy [34,35], nuclear magnetic resonance spectroscopy [34,36,37], fluorescence spectrometry [22], neutron scattering [38] and positron annihilation [39] measurements.

The present study utilizes Raman spectroscopy to examine the temperature-dependent behavior of the bonded ligands of a 3.52 and a 2.34 μmol m^{-2} Microporasil C_{18} stationary phase equilibrated in

different mobile phase environments. This study represents the first time that both the mobile phase composition and the temperature are simultaneously controlled to examine silica-bonded octadecylsilyl (C_{18}) ligands spectroscopically at typical liquid chromatographic (LC) mobile phase flow-rates and back pressures. Raman spectroscopy is used to characterize the behavior of the C_{18} bonded ligands equilibrated at temperatures from 2 to 45°C in neat, single-component, mobile phase solvents including: water, acetonitrile, methanol, and chloroform. In addition, the effect of stationary phase ligand bonding density is also examined by using two different monomeric reversed-phase liquid chromatographic (RPLC) stationary phases, 2.34 and 3.52 μmol m^{-2} Microporasil C_{18} stationary phases, under identical conditions. The direct, on-column, spectroscopic analysis used in this study allows direct evaluation of the temperature-dependent behavior of the bonded C_{18} ligands. The temperature-dependent ordering of the stationary phase ligands is examined to determine if the ligands undergo a phase transition from a less-ordered ''liquid-like'' state at higher temperatures to a more-ordered ''solid-like'' state at lower temperatures.

2. Experimental

The same experimental setup, stationary phases, and mobile phases are being used as in the previous paper [40], with the exception that the phase transition behavior of neat octadecane (99% purity: Aldrich Chemical Company, Milwaukee, WI, USA) is also investigated to assist in the interpretation of the results obtained for the bonded phases. For each of the spectra in this work, the features due to the fiber-optic probe [41] and to the individual mobile phases [40] have already been subtracted.

3. Results and discussion

3.1. Temperature effects on features of octadecane, and C_{18} ligands in the presence of water

Fig. 1 displays the spectral features obtained for solid (Spectrum a) and liquid (Spectrum c) neat octadecane at 2 and 35°C, respectively. Corresponding bonded octadecylsilyl (C_{18}) ligand spectral features at 2 (Spectrum b) and 35°C (Spectrum d) are also presented in this figure. These bonded phase spectra were obtained using the 3.52 μmol m^{-2} Microporasil C_{18} stationary phase, and the features of the 100% aqueous mobile phase in which the stationary phase ligands were equilibrated have already been subtracted. Spectral features of the carbon–carbon stretching (C–C stretching) and the carbon–hydrogen bending (C–H bending) region (low wavenumber region) are shown in Fig. 1A, whereas spectral features of the carbon–hydrogen stretching (C–H stretching) region (high wavenumber region) are shown in Fig. 1B.

An initial comparison of the spectral features due to solid (Spectrum a) and liquid (Spectrum c) octadecane is a convenient starting point. In the low wavenumber region (Fig. 1A), characteristic bands [42,43] due to carbon–carbon–carbon symmetric stretching at 891 cm^{-1} [ν_s (CCC)]; asymmetric and symmetric carbon–carbon stretching of the hydrocarbon chains in the ''trans'' conformation at about 1059 cm^{-1} [ν_a $(C–C)_T$] and about 1130–1133 cm^{-1} [ν_s $(C–C)_T$], respectively; carbon–carbon stretching of the hydrocarbon chains in ''gauche'' conformations at about 1079 cm^{-1} [ν $(C–C)_G$]; methylene in-phase twisting [τ (CH_2)] at about 1294–1300 cm^{-1}; methyl symmetric and asymmetric bending at 1366 cm^{-1} [δ_s (CH_3)] and at about 1438–1445 cm^{-1} [δ_a (CH_3)], respectively; and methylene scissoring [δ_{sci} (CH_2)] at about 1448–1462 cm^{-1} are evident in the spectra of solid (Spectrum a) and liquid (Spectrum c) neat octadecane.

Comparison of the band shapes and relative intensities of selective bands observed for solid and liquid octadecane demonstrates, not too surprisingly, that Raman spectroscopic measurements are sensitive to the physical state of neat alkanes. First, note that several bands, including the ν_a $(C–C)_T$, ν_s $(C–C)_T$, and τ (CH_2) bands, are much narrower and more intense for solid octadecane than for liquid octadecane. This narrowing of the different bands is indicative of octadecane undergoing a transition from a less ordered liquid state to a more-ordered solid state. In fact, the ''trans'' chain conformation of alkanes, indicates that the carbons within the chain are in their most ordered, linear configuration, as

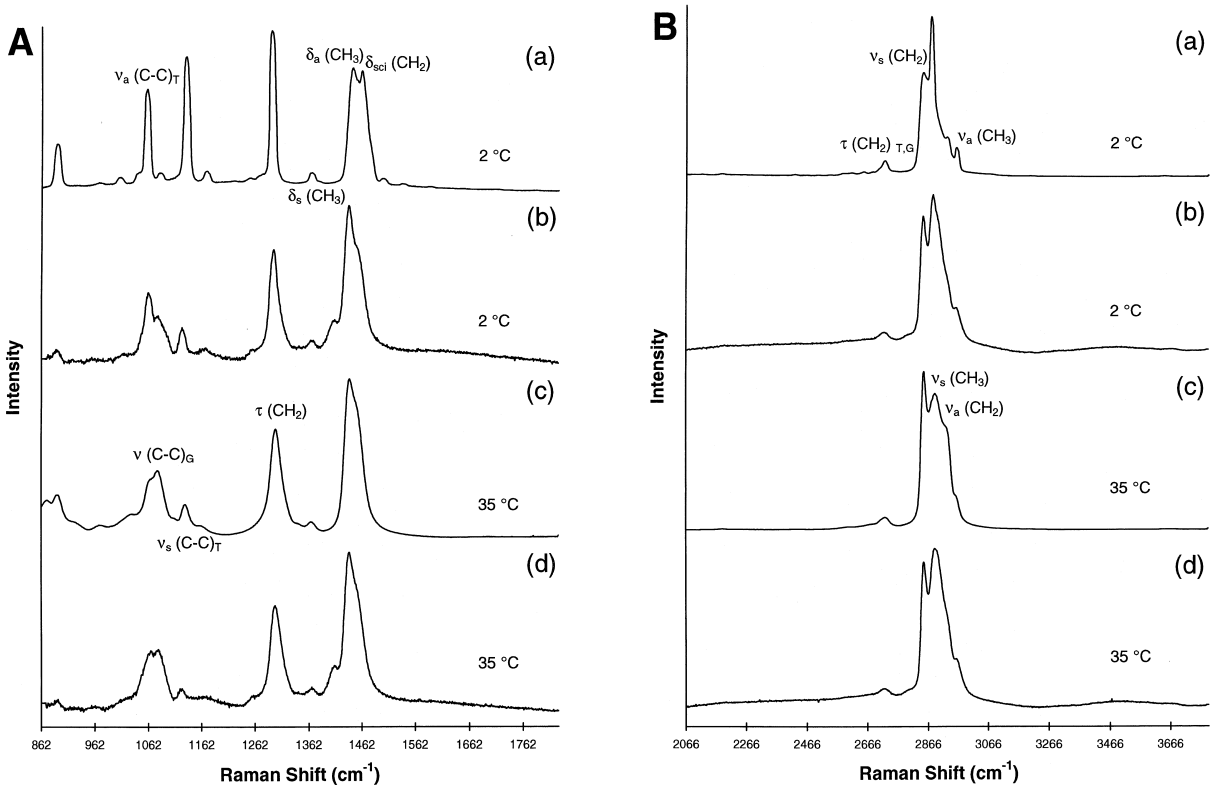

Fig. 1. (A) Spectral features in the C–C stretching and C–H bending region due to (a) neat solid octadecane at 2°C; (b) the bonded ligands of the 3.52 μmol m^{-2} Microporasil C$_{18}$ stationary phase at 2°C, with water mobile phase features subtracted; (c) neat liquid octadecane at 35°C; and (d) the bonded ligands of the 3.52 μmol m^{-2} Microporasil C$_{18}$ stationary phase at 35°C, with water mobile phase features subtracted. The spectra have been multiplied by the following scaling factors: (a) ×1, (b) ×16.98, (c) ×1.730, (d) ×18.36. (B) Same as (A), except that the spectral region is the C–H stretching region. Spectral scaling factors: (a) ×1.169, (b) ×8.378, (c) ×1, (d) ×9.213.

opposed to various ''gauche'' configurations in which the chain can have a number of kinks and/or bends that arranges the alkane chain in non-linear orientations. The relative intensities of the ν_a (C–C)$_T$, ν_s (C–C)$_T$, and ν (C–C)$_G$ bands are sensitive to these configurational changes, and indicate that more of the alkane chains are in disordered gauche configurations for liquid octadecane (Spectrum c), whereas as a substantially higher proportion of the alkane chains are in the more-ordered trans configuration for solid octadecane (Spectrum a). Also, the peak maximum of the ν_s (C–C)$_T$ band shifts from 1130 cm^{-1} for liquid (Spectrum c) to 1133 cm^{-1} for solid (Spectrum a) octadecane.

Another noticeable difference between the spectra of liquid and solid octadecane in the low wavenumber region (Fig. 1A) is that for solid octadecane (Spectrum a), there are two overlapped, but nonetheless distinct bands due to δ_a (CH$_3$) at 1445 cm^{-1} and δ_{sci} (CH$_2$) at 1462 cm^{-1}, whereas these bands have appeared to coalesce into a seemingly single band at 1438 cm^{-1} for liquid octadecane. This ''single'' band was previously referred to as the δ_a (CH$_3$)/δ_{sci} (CH$_2$) band for the alkyl bonded stationary phases [40,41]. Note that in the case of liquid octadecane (Spectrum c), this δ_a (CH$_3$)/δ_{sci} (CH$_2$) band is more intense than the τ (CH$_2$) band, whereas the τ (CH$_2$) band is more intense than the δ_a (CH$_3$) and δ_{sci} (CH$_2$) overlapped features for solid octadecane (Spectrum a). Further, the peak maximum of the τ (CH$_2$) band has also shifted from 1300 cm^{-1} for liquid (Spectrum c) to 1294 cm^{-1} for solid (Spectrum a) neat octadecane.

In the case of the bonded phase features in the low

wavenumber region (Spectra b and d of Fig. 1A), the C–C stretching region is also indicative of chain ordering for the bonded phase C_{18} ligands. The ν_a $(C–C)_T$ and ν_s $(C–C)_T$ bands are more intense for the bonded phase at 2°C (Spectrum b) than for the same bonded phase at 35°C (Spectrum d), although there is still considerable intensity in the ν $(C–C)_G$ region of both the spectra. Previous studies were conducted at ambient temperature [41] and at 35°C [40], and so the region encompassing the ν_a $(C–C)_T$ and ν $(C–C)_G$ features was identified as the ν_a (C–C) region because, as is observed in Spectrum d, it is not readily apparent that more than one band is present at the higher temperatures. This is especially true considering the prominence of the silica fiber-optic probe features in this region [41], which, as previously mentioned, have already been subtracted from the spectra presented here. The bonded phase spectra (Spectra b and d) contain the additional shoulder at about 1409 cm^{-1} due to the methyl-silicon deformations [δ $(Si–CH_3)$] of the di-methylsilyl moiety that connects the octadecyl chain to the silica surface [41]. Also noticeable in the C–H bending region for the C_{18} bonded phase ligands (Spectra b and d), is that the δ_a $(CH_3)/\delta_{sci}$ (CH_2) band is narrower and more apparently the result of an overlap of multiple features at 2°C (Spectrum b) than at 35°C (Spectrum d). The spectral features of the bonded C_{18} ligands (Spectra b and d) in the low wavenumber region (Fig. 1A) indicate that temperature changes influence the configurations of the bonded ligands, although not as drastically as for neat octadecane (Spectra a and c). In addition, the bonded ligands appear to behave very similarly to liquid octadecane at both 2 and 35°C, as evidenced by the fact that the ligand features more closely resemble those of liquid than solid octadecane. The resemblance of the bonded C_{18} ligand features to liquid octadecane may be surprising because the motionally-restricted surface-attached (grafted) ligands are spaced too far apart to interact with one another in a truly liquid fashion.

In the high wavenumber region (Fig. 1B), there are again considerable differences between the spectral features of solid (Spectrum a) and liquid (Spectrum c) neat octadecane. Characteristic bands [42,43] due to methylene twisting [τ $(CH_2)_{T,G}$] at 2723 cm^{-1}; methylene symmetric and asymmetric stretching at about 2850–2853 cm^{-1} [ν_s (CH_2)] and about 2923–2929 cm^{-1} [ν_a (CH_2)], respectively; and methyl symmetric and asymmetric stretching at about 2879–2890 cm^{-1} [ν_s (CH_3)] and 2960 cm^{-1} [ν_a (CH_3)], respectively, are present in both spectra of octadecane. Methylene symmetric and asymmetric stretching is considerably more prominent for liquid (Spectrum c) than for solid (Spectrum a) neat octadecane. Narrowing of spectral features, which is again indicative of chain ordering, is evident for solid octadecane. The drastic reduction of methylene asymmetric stretching combined with the apparent narrowing of the methyl symmetric stretching band for solid octadecane (Spectrum a) have considerably reduced the spectral intensity in the region between about 2890 and 2953 cm^{-1}, in comparison to liquid octadecane (Spectrum c).

The spectral features of the 3.52 μmol m^{-2} C_{18} ligands at both 2 (Spectrum b) and 35°C (Spectrum d) again more closely resemble those of liquid (Spectrum c) than solid (Spectrum a) octadecane in the C–H stretching region (Fig. 1B), although the agreement of the C_{18} bonded phase features with liquid octadecane is not as good as it was in the low wavenumber region (Fig. 1A). The major difference between the spectral features of liquid octadecane (Spectrum c) and the bonded C_{18} ligands (Spectra b and d) is that both methylene symmetric and asymmetric stretching bands are considerably more prominent for liquid octadecane than for the bonded ligands. This reduced methylene stretching of the bonded ligands most probably results from the restricted motion of the methylene groups upon anchoring the octadecylsilyl ligands to the silica surface. Comparison of the bonded C_{18} ligand spectral features at 2 (Spectrum b) and 35°C (Spectrum d) again indicates that the spectral features are sensitive to changes in temperature. In particular, the ν_s $(CH_3)/\nu_a$ (CH_2) band is narrower at 2°C (Spectrum b) than at 35°C (Spectrum d), and the peak maximum has shifted from 2889.7 cm^{-1} at 35°C to 2883.7 cm^{-1} at 2°C. This band narrowing is again indicative of the ligands becoming more ordered, but again the spectral features do not change as drastically for the bonded C_{18} ligands as they do for neat octadecane.

Examination of spectral features within narrower regions, and the superimposition of spectral features

allows further comparisons to be made. The spectral features of the 3.52 μmol m^{-2} C_{18} stationary phase ligands at 2 and 35°C (as well as at 12.5°C in the C–H stretching region (Fig. 2B)) are superimposed in Spectra a, whereas those of solid (2°C) and liquid (35°C) octadecane are superimposed in Spectra b in both the C–H bending region (Fig. 2A) and the C–H stretching region (Fig. 2B). As was discussed in conjunction with the spectral features of neat octadecane in Fig. 1A, the τ (CH_2) band of solid octadecane (2°C) is narrower, of higher relative intensity, and is shifted to lower energy by about 6 cm^{-1} (Spectra b of Fig. 2A) in comparison to that of liquid octadecane (35°C). In addition, the δ_a (CH_3) and δ_{sci} (CH_2) bands are also changed. For solid octadecane these appear at 1445 and 1462 cm^{-1}, respectively. For liquid octadecane these appear as a single more intense band at 1438 cm^{-1} with a shoulder at roughly 1448 cm^{-1}.

As was also previously discussed in conjunction with the bonded C_{18} ligand features in Fig. 1A, and which is now more readily observed (Spectra a of Fig. 2A), the δ_a (CH_3)/δ_{sci} (CH_2) band is narrower at 2°C and the shoulder due to methylene scissoring is also more evident than at 35°C. Also, it is now apparent in the superimposed spectra, that the τ (CH_2) band is also temperature sensitive in the case of the bonded C_{18} ligands (Spectra a of Fig. 2A). The τ (CH_2) band is again narrower, of higher relative intensity, and is shifted to lower energy by 2.5 cm^{-1} for the bonded C_{18} ligands at 2°C in comparison to 35°C. What is interesting to note is

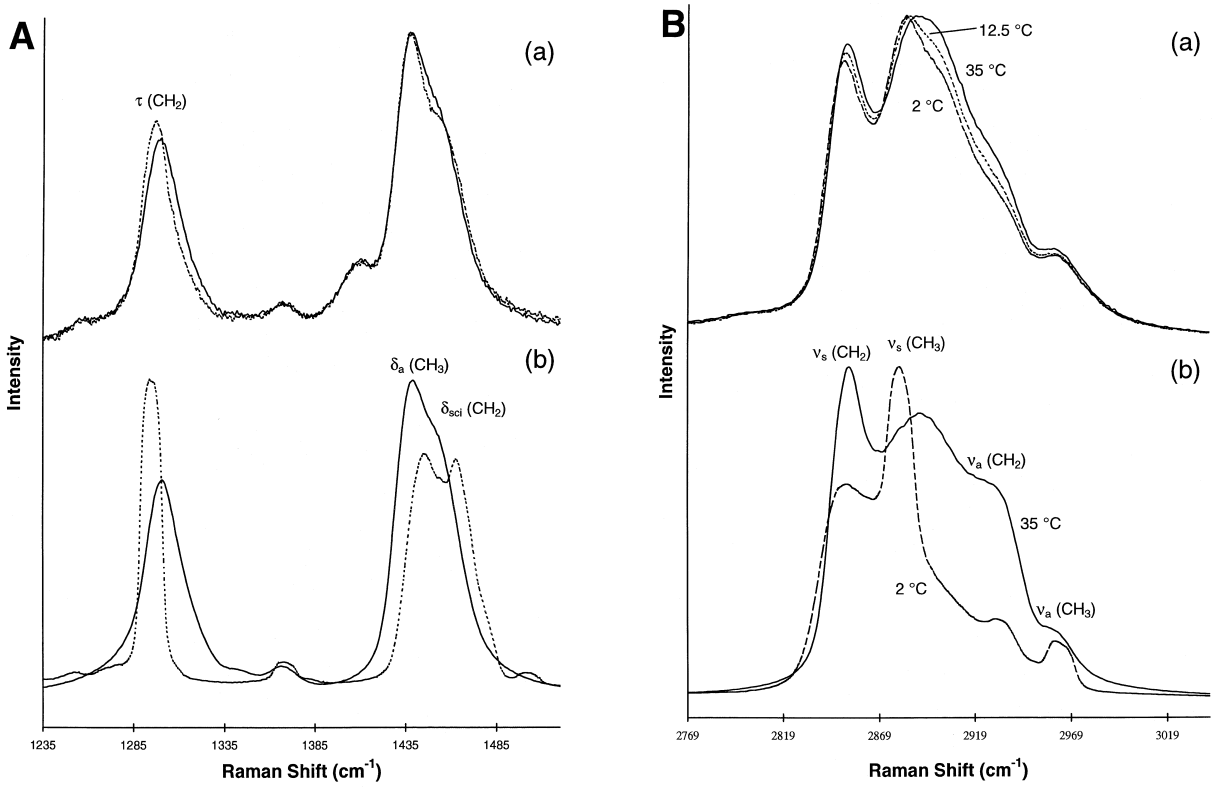

Fig. 2. (A) Superimposition of spectral features in the C–H bending region due to (a) the bonded ligands of the 3.52 μmol m^{-2} Microporasil C_{18} stationary phase at 2 (- - -) and 35 (—)°C, with water mobile phase features subtracted, and (b) neat octadecane at 2 (- - -) and 35 (—)°C. Spectral scaling factors: (a) ×16.98 at 2°C and ×18.36 at 35°C; (b) ×1 at 2°C and ×1.730 at 35°C. (B) Superimposition of spectral features in the C–H stretching region due to (a) the bonded ligands of the 3.52 μmol m^{-2} Microporasil C_{18} stationary phase at 2 (- - -), 12.5 (· · ·), and 35 (—)°C, with water mobile phase features subtracted, and (b) neat octadecane at 2 (- - -) and 35 (—)°C. Spectral scaling factors: (a) ×8.378 at 2°C, ×8.882 at 12.5°C, and ×9.213 at 35°C; (b) ×1.169 at 2°C and ×1 at 35°C.

that, although the changes are more subtle, the behavior of the τ (CH_2) band with temperature changes is similar for the bonded C_{18} ligands and neat octadecane. On the other hand, the δ_a (CH_3)/δ_{sci} (CH_2) band of the bonded C_{18} ligands narrows toward lower energy in going to lower temperature, but both the δ_a (CH_3) and δ_{sci} (CH_2) bands shift in the opposite direction to higher energy at the lower temperature (2°C) for neat octadecane.

In the C–H stretching region (Fig. 2B), the changes that occur for octadecane in going from a solid (2°C) to a liquid (35°C) are readily apparent upon spectral superimposition (Spectra b). The narrowing of the spectral features within the region between 2890 and 2953 cm^{-1} can be seen in going from liquid (35°C) to solid (2°C) neat octadecane. The spectral features due to the bonded C_{18} ligands in Spectra a (Fig. 2B) follow a similar trend to that of neat octadecane in that the ν_s (CH_3) and ν_a (CH_2) features become narrower, and the peak maximum shifts to lower energy: from 2889.7 to 2885.2 to 2883.7 cm^{-1} in going from 35 to 12.5 to 2°C, respectively, for the bonded C_{18} ligands. Also like octadecane, the ν_s (CH_2) band due to the bonded C_{18} ligands decreases in intensity relative to the ν_s (CH_3) band and again shifts to slightly lower energy: from 2851.9 to 2850.3 cm^{-1} in going from 35 down to 2°C. However, this gradual narrowing of the spectral features due to bonded C_{18} ligands in going to lower and lower temperatures is different than the behavior of the spectral features observed for neat octadecane. Neat octadecane undergoes a discrete phase transition whereby the spectral features observed above (45 and 35°C), and below (25, 12.5 and 2°C), the phase transition temperature (28–30°C) are superimposable.

The susceptibility of bonded phase spectral features to changes in temperature is more clearly seen in Fig. 3, which shows the 3.52 μmol m^{-2} C_{18} stationary phase ligand spectral features with H_2O mobile phase features subtracted. The spectral features of the 2.34 μmol m^{-2} C_{18} stationary phase exhibited similar behavior in an aqueous environment, and are therefore not shown. In the C–C stretching and C–H bending region (Fig. 3A), the ν_a $(C–C)_T$ and ν_s $(C–C)_T$ bands become increasingly more prominent and the narrowing of the δ_a (CH_3)/δ_{sci} (CH_2) band becomes increasingly more noticeable as the temperature is progressively decreased from 45, 35, 25, 12.5 down to 2°C, with these changes being more readily apparent at 25°C and below. The progressive narrowing of the δ_a (CH_3)/δ_{sci} (CH_2) band with decreasing temperature is more obvious upon superimposing the spectra in the C–H bending region (Fig. 3B).

Also evident in the C–H bending region is the general trend of a progressive increase in the intensity of the τ (CH_2) band and the gradual shift of this peak maximum to lower energy with decreasing temperature for both the 3.52 μmol m^{-2} (Fig. 3B) and the 2.34 μmol m^{-2} (not shown) C_{18} stationary phases. The seemingly anomalous behavior at 12.5°C for the 3.52 μmol m^{-2} C_{18} phase (Fig. 3B) could, in part, be due to differences in background intensity. For instance, the spectral features at 12.5°C are lower in intensity than at any other temperature in the spectral region between 1490 and 1520 cm^{-1}, whereas they are the features of highest intensity than at any other temperature in the δ_s (CH_3) region, the region from about 1235 to 1270 cm^{-1}, as well as in the τ (CH_2) region.

Another contributing factor, especially in the location of the peak maximum of the τ (CH_2) band at 1298.3 cm^{-1} for the features at 12.5°C (Fig. 3B), appears to result from the skewing of the shape of the τ (CH_2) band at 12.5°C (Fig. 3A) in comparison to the more symmetric, almost Gaussian, τ (CH_2) bands at 45, 35 and 25°C. No explanation, assignable to a specific phenomenon or event, for this apparent discrepancy in peak shape is available at this time. However, although the τ (CH_2) band at 2°C is not nearly as distorted as at 12.5°C, particularly not at the peak maximum (Fig. 3B), the overall band shape appears to be slightly more asymmetric, like at 12.5°C, than at 45, 35, and 25°C. In addition, the narrowing of the τ (CH_2) band at 2°C discussed in conjunction with Spectrum a of Fig. 2A, does not appear to have occurred at the other temperatures for the 3.52 μmol m^{-2} C_{18} phase (Fig. 3B) or for any of the temperatures in the case of the 2.34 μmol m^{-2} C_{18} phase (not shown). This seemingly anomalous behavior at 2°C for the 3.52 μmol m^{-2} C_{18} phase will be addressed in the discussion of the bonded C_{18} ligand spectral features obtained from other mobile phase solvents.

As was previously discussed (Spectra a of Fig.

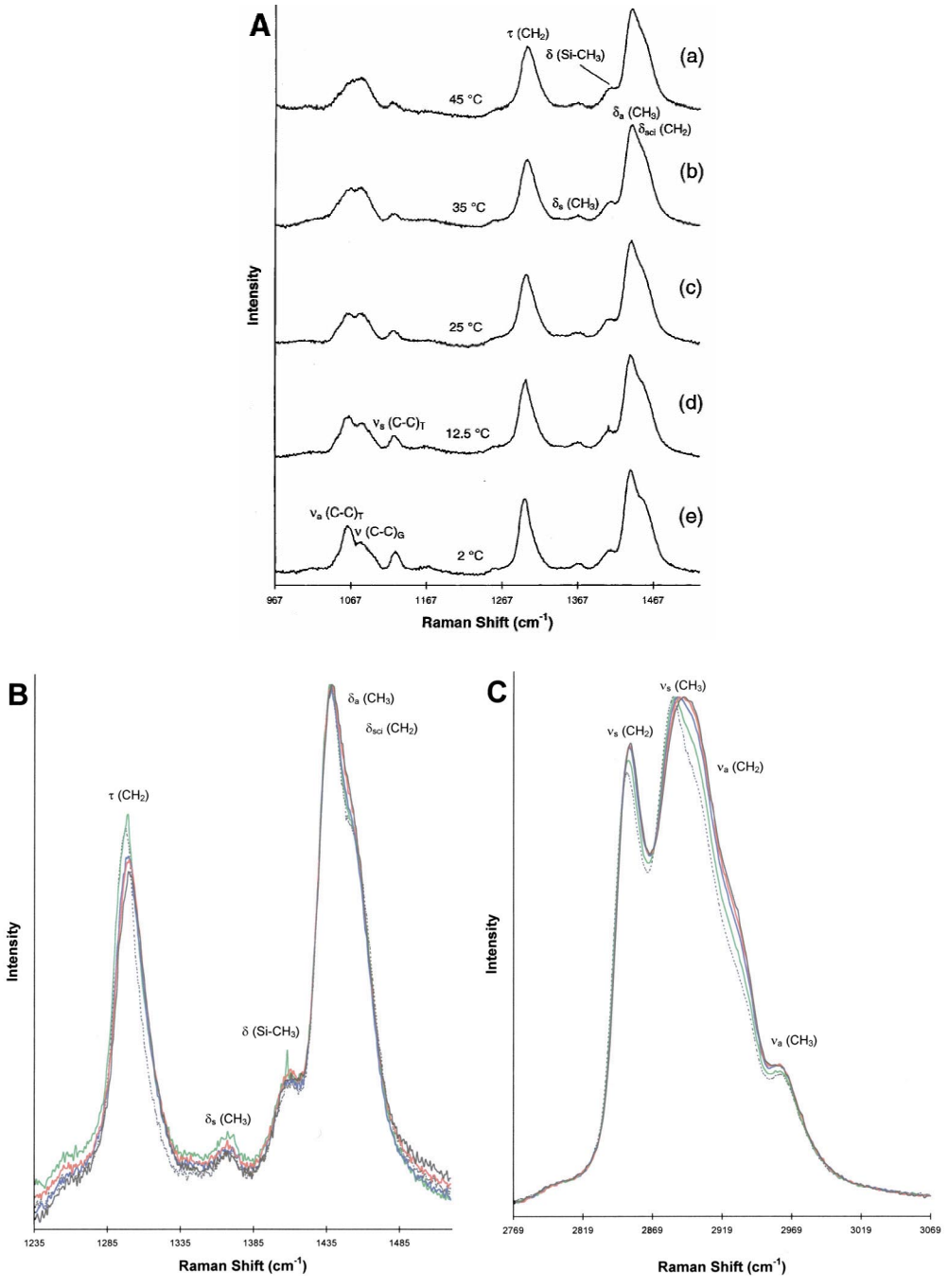

Fig. 3. (A) Spectral features in the C–C stretching and C–H bending region due to the bonded ligands of the 3.52 μmol m^{-2} Microporasil C_{18} stationary phase, after removal of water mobile phase features, at (a) 45°C (×1.217), (b) 35°C (×1.048), (c) 25°C (×1.018), (d) 12.5°C (×1.021), and (e) 2°C (×1). (B) Superimposition of spectral features in the C–H bending region due to the bonded ligands of the 3.52 μmol m^{-2} Microporasil C_{18} stationary phase, with water mobile phase features subtracted, at 45°C (black, ×1.217), 35°C (red, ×1.059), 25°C (blue, ×1.018), 12.5°C (green, ×1.049), and 2°C (black dash - - -, ×1). (C) Same as (B), except that the spectral region is the C–H stretching region. Spectral scaling factors: 45°C (×1.118), 35°C (×1.099), 25°C (×1.069), 12.5°C (×1.057), and 2°C (×1).

2B), the ν_s $(CH_3)/\nu_a$ (CH_2) band becomes narrower, the intensity of the ν_s (CH_2) decreases, and both bands generally shift to lower energy with decreasing temperature from 45, 35, 25, 12.5 down to 2°C, for the bonded ligands of both the 3.52 (Fig. 3C) and the 2.34 (not shown) μmol m^{-2} C_{18} phases. The ν_s $(CH_3)/\nu_a$ (CH_2) band shifts from 2892.7 cm^{-1} for the 2.34 μmol m^{-2} C_{18} phase and 2891.2 cm^{-1} for the 3.52 μmol m^{-2} C_{18} phase at 45°C down to 2883.7 cm^{-1} at 2°C for both phases. With the exception of the 2.34 μmol m^{-2} C_{18} phase at 45°C, the ν_s (CH_2) band intensity decreases with decreasing temperature, and shifts from 2853.4 cm^{-1} at 45°C down to 2850.3 cm^{-1} at 2°C for both phases. The slightly decreased intensity of the ν_s (CH_2) band relative to the ν_s $(CH_3)/\nu_a$ (CH_2) band at 45°C for the 2.34 μmol m^{-2} C_{18} phase, in comparison to the intensity observed at 35 and 25°C (not shown), is largely due to differences in the backgrounds of the spectra.

3.2. Temperature effects on C_{18} ligand features in the presence of ACN and MeOH

As noted in the preceding article [40], subtraction of the spectral features due to the acetonitrile and methanol mobile phases from the features of the C_{18} ligands is difficult, and residual solvent features are typically still evident in the spectra of the bonded phase C_{18} ligands. This is especially true for the 2.34 μmol m^{-2} Microporasil C_{18} stationary phase since fewer alkyl ligands are contributing to the bonded ligand spectral intensity than for the 3.52 μmol m^{-2} Microporasil C_{18} phase. Nonetheless, examination of the spectral features due to the bonded ligands of the 3.52 μmol m^{-2} Microporasil C_{18} stationary phase as a function of temperature, with the ACN (Fig. 4) and MeOH (Fig. 5) mobile phase features subtracted, is still informative.

In the C–C stretching and C–H bending region, the ν_a $(C–C)_T$ and ν_s $(C–C)_T$ bands are more prominent at 2°C than at 35°C, and the δ_a $(CH_3)/\delta_{sci}$ (CH_2) band appears to be only slightly more narrow at the lower temperature for the 3.52 μmol m^{-2} C_{18} ligand features obtained from ACN (Fig. 4A). In the case of the 3.52 μmol m^{-2} C_{18} ligand features obtained from MeOH in the low wavenumber region (Fig. 5A), residual carbon–oxygen stretching and methyl bending features due to MeOH, in the 995 to 1050 cm^{-1} and 1420 to 1530 cm^{-1} spectral regions respectively, obscure the bonded C_{18} ligand features in these regions, particularly at 2°C. Nonetheless, the ν_s $(C–C)_T$ band, and even the ν_a $(C–C)_T$ band, appear to be more prominent at 2°C than at 35°C (Fig. 5A).

Superimposition of the bonded C_{18} ligand spectral features obtained from ACN in the C–H bending region (Fig. 4B) allows the subtle narrowing of the δ_a $(CH_3)/\delta_{sci}$ (CH_2) band at 2°C to be observed. In addition, although the backgrounds of the spectral features observed at 2 and 35°C differ slightly, not only is the increased intensity and the shift to lower energy of the τ (CH_2) band at the lower temperature observed, but this band also appears to be more narrow at 2°C than at 35°C. This result indicates that the narrowing of the τ (CH_2) band at 2°C for the 3.52 μmol m^{-2} C_{18} ligand features obtained from H_2O (Figs. 2A and 3B) is not an anomalous occurrence, but rather appears to be a repeatable phenomenon. This is further substantiated by the observance of the same narrowing behavior of the τ (CH_2) band for the 3.52 μmol m^{-2} C_{18} bonded ligand spectral features at 2°C obtained from MeOH (Fig. 5B). The narrowing of the δ_a $(CH_3)/\delta_{sci}$ (CH_2) features in Fig. 5B, however, do not indicate bonded phase changes with temperature, especially since the spectral features at 35°C are more narrow than those at 2°C, but rather that the presence of a greater amount of residual MeOH features is present at 2°C than at 35°C, as was also indicated in Fig. 5A.

The increased order of the stationary phase ligands at lower temperature is again indicated by the bonded ligand spectral features in the C–H stretching region obtained from both ACN (Fig. 4C) and MeOH (Fig. 5C). Although the spectral region between about 2927 and 2959 cm^{-1} is distorted by subtraction difficulties [40] and the methyl asymmetric stretching band due to residual ACN is still evident in Fig. 4C, and the fact that the prominence and width of the ν_a (CH_3) band in Fig. 5C is indicative of residual MeOH [40], the C_{18} bonded ligand features still exhibit similar changes with temperature as was observed for the bonded ligand features obtained from H_2O. The ν_s $(CH_3)/\nu_a$ (CH_2) band due to the bonded C_{18} ligands shifts from

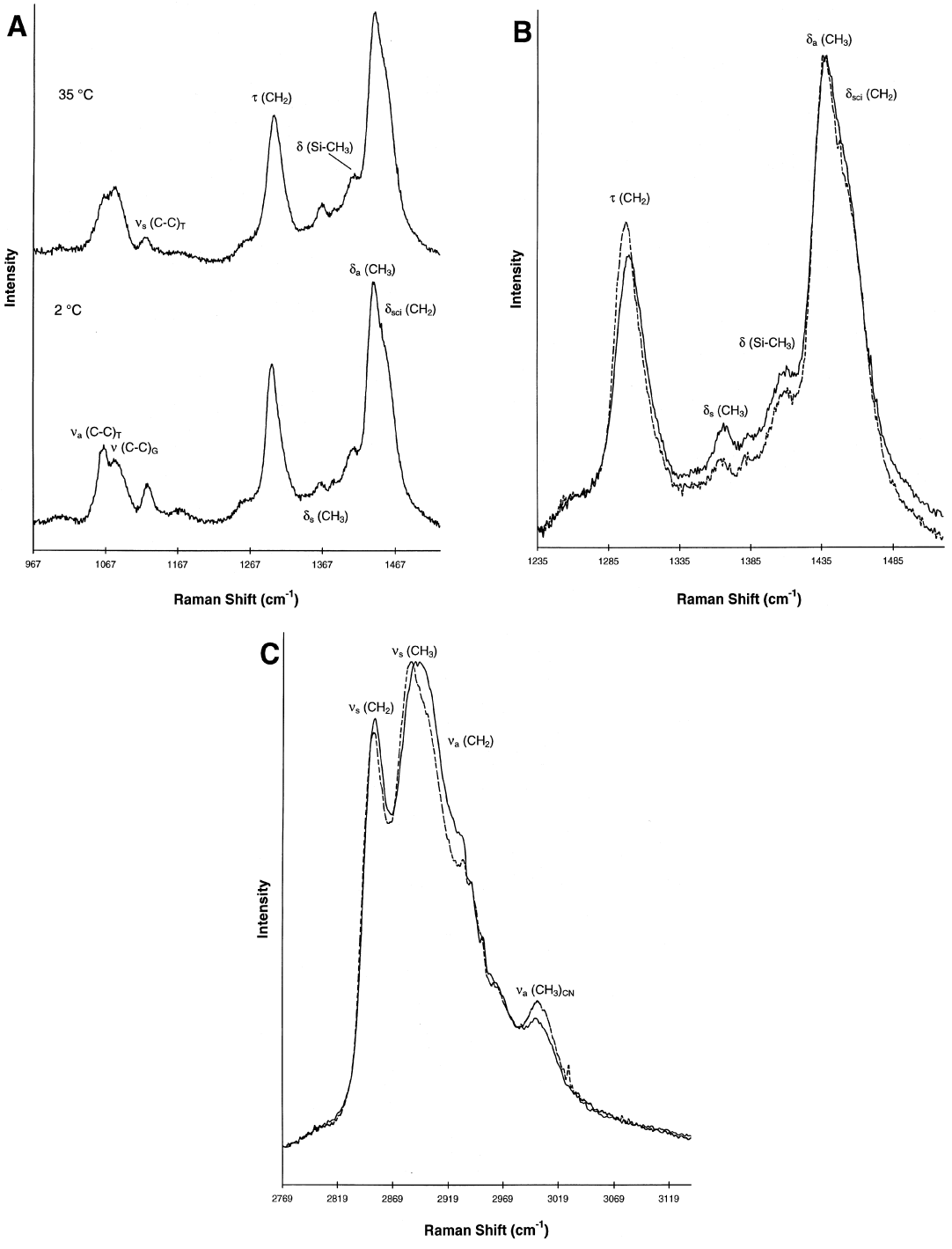

Fig. 4. (A) Effect of temperature on the spectral features due to the bonded ligands of the 3.52 μmol m^{-2} Microporasil C_{18} stationary phase, with acetonitrile mobile phase features subtracted, in the C–C stretching and C–H bending region at 35 (—, ×1) and 2 (- - -, ×1.068)°C. (B) Same as (A), except that the spectral region is the C–H bending region. Spectral scaling factors: 35°C (×1), 2°C (×1.112). (C) Same as (A), except that the spectral region is the C–H stretching region. Spectral scaling factors: 35°C (×1), 2°C (×1.006).

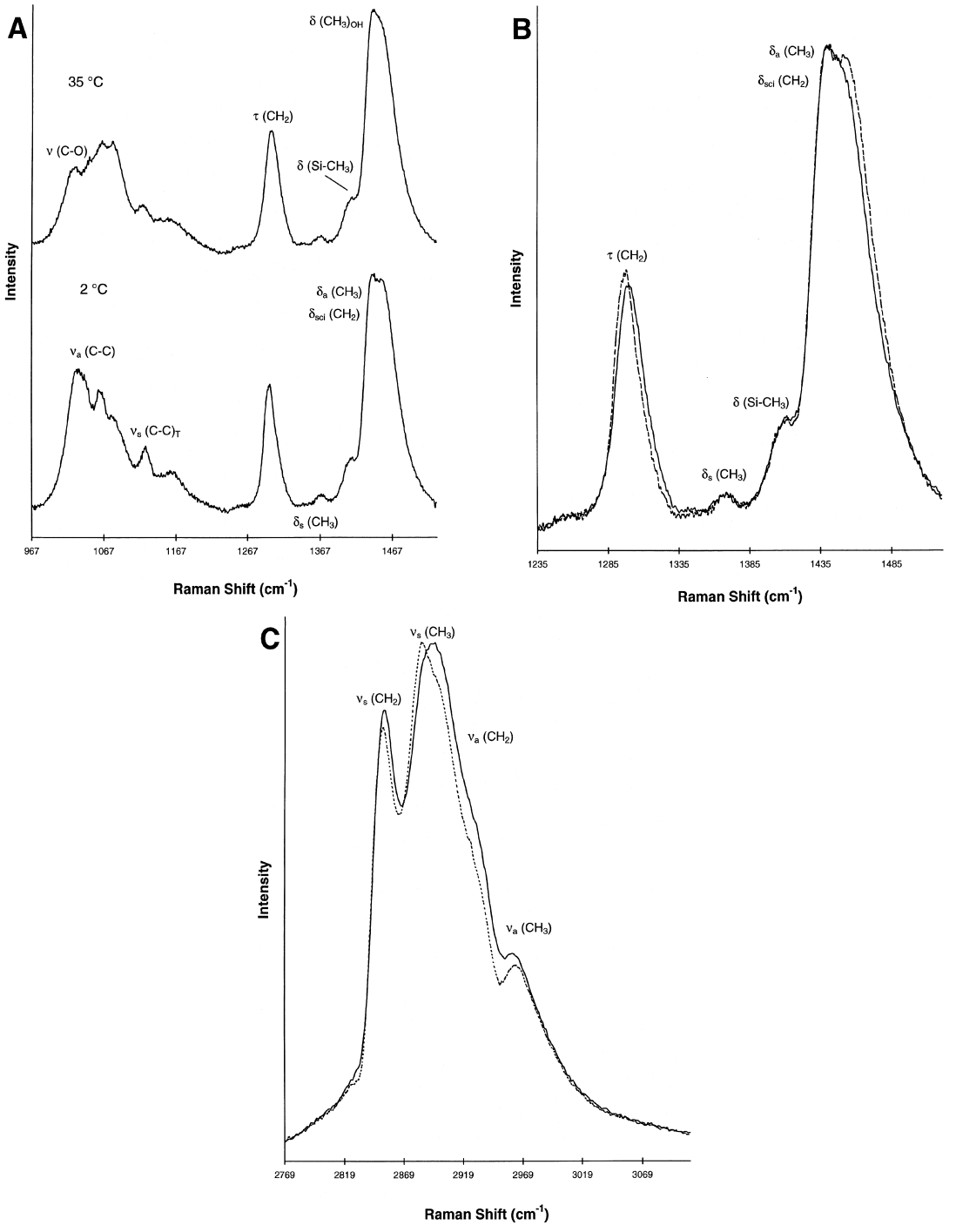

Fig. 5. (A) Effect of temperature on the spectral features due to the bonded ligands of the 3.52 μmol m^{-2} Microporasil C_{18} stationary phase, with methanol mobile phase features subtracted, in the C–C stretching and C–H bending region at 35 (—, ×1.092) and 2 (- - -, ×1)°C. (B) Same as (A), except that the spectral region is the C–H bending region. Spectral scaling factors: 35°C (×1.069), 2°C (×1). (C) Same as (A), except that the spectral region is the C–H stretching region. Spectral scaling factors: 35°C (×1.068), 2°C (×1).

2889.7 to 2885.2 cm^{-1} upon decreasing the equilibration temperature from 35 to 2°C for the ligand features obtained from ACN (Fig. 4C), and from 2895.8 to 2883.7 cm^{-1} for the ligand features obtained from MeOH (Fig. 5C) under the same temperature conditions. In both solvent environments (Figs. 4C and 5C) the ν_s (CH_2) band decreases in intensity and shifts from about 2853.4 to 2851.9 cm^{-1} in going from 35 to 2°C.

3.3. Temperature effects on C_{18} ligand features in the presence of $CHCl_3$

Chloroform, like water, is a spectroscopically convenient mobile phase because its spectral features do not drastically overlap the features due to the C_{18} bonded phase ligands [40]. The spectral features due to the 3.52 and the 2.34 μmol m^{-2} C_{18} phases equilibrated in neat $CHCl_3$ mobile phases, with the $CHCl_3$ spectral features already subtracted, are shown in Figs. 6 and 7, respectively. In the C–C stretching and C–H bending region, the ν_a $(C–C)_T$ and ν_s $(C–C)_T$ bands are slightly more prominent at 2°C than at 35°C for the 3.52 μmol m^{-2} C_{18} phase (Fig. 6A), but the spectral features due to the 2.34 μmol m^{-2} C_{18} phase (Fig. 7A) are considerably more noisy and there do not appear to be any readily noticeable differences due to temperature changes in this spectral region. The δ_a $(CH_3)/\delta_{sci}$ (CH_2) and τ (CH_2) bands of both stationary phases exhibit spectral changes with temperature similar to what was observed for the bonded ligands in H_2O, ACN, and MeOH, although the ligand spectral changes are not as dramatic in $CHCl_3$. In each of the $CHCl_3$-subtracted spectra in the low wavenumber region (Figs. 6A and 7A), distortions in the region from about

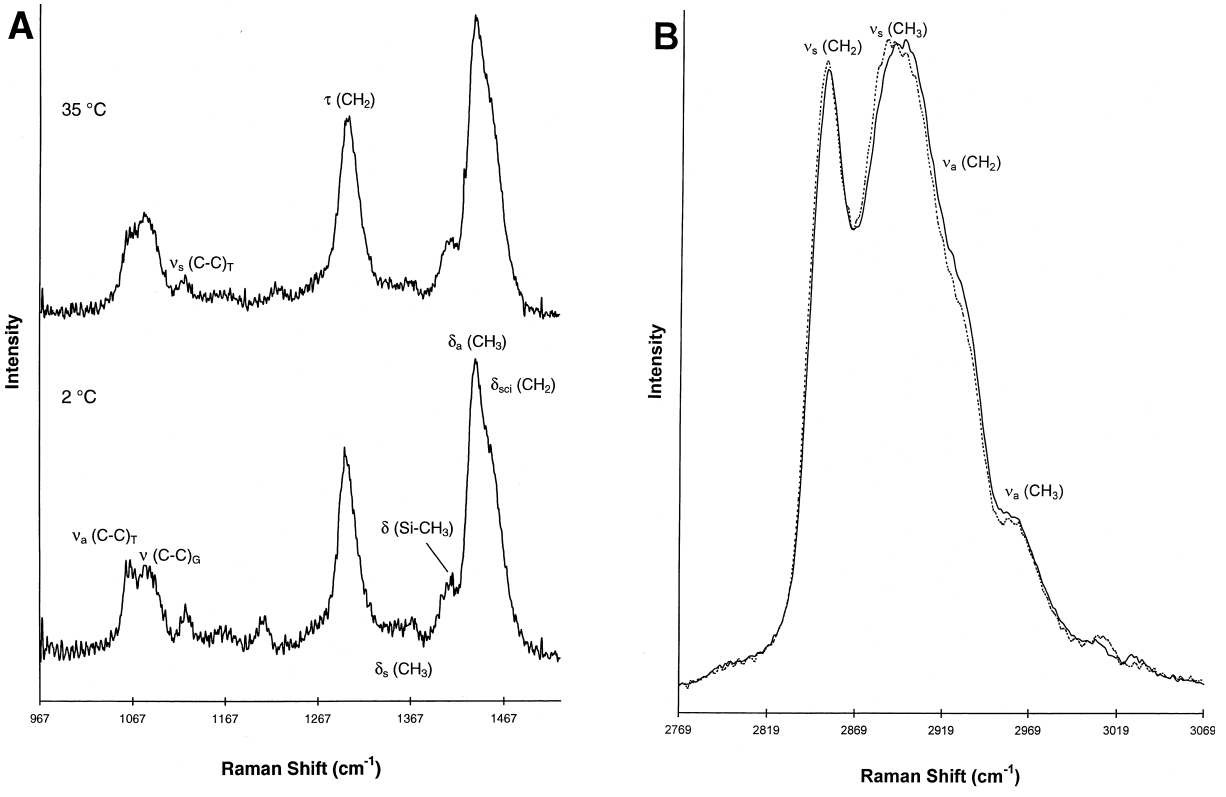

Fig. 6. (A) Effect of temperature on the spectral features due to the bonded ligands of the 3.52 μmol m^{-2} Microporasil C_{18} stationary phase, with chloroform mobile phase features subtracted, in the C–C stretching and C–H bending region at 35 (—, ×1.210) and 2 (- - -, ×1)°C. (B) Same as (A), except that the spectral region is the C–H stretching region. Spectral scaling factors: 35°C (×1.148), 2°C (×1).

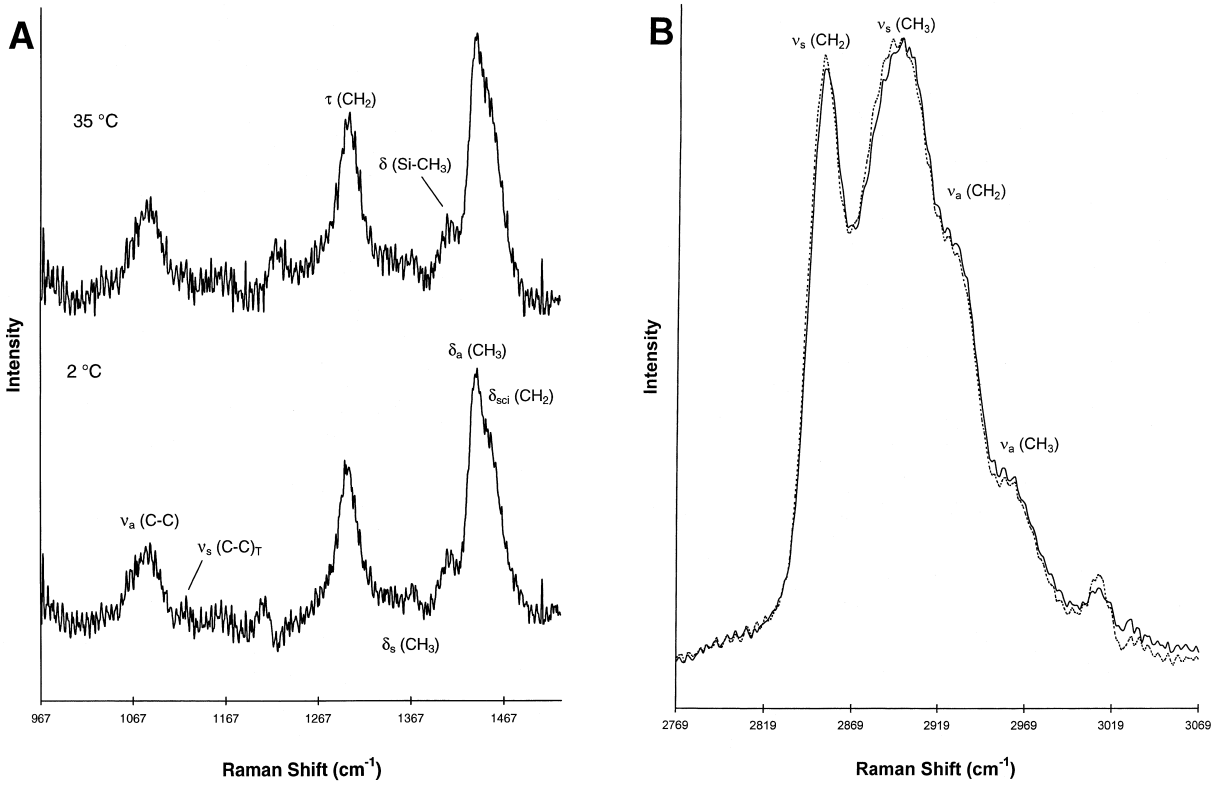

Fig. 7. (A) Effect of temperature on the spectral features due to the bonded ligands of the 2.34 μmol m^{-2} Microporasil C_{18} stationary phase, with chloroform mobile phase features subtracted, in the C–C stretching and C–H bending region at 35 (—, ×1) and 2 (- - -, ×1.065)°C. (B) Same as (A), except that the spectral region is the C–H stretching region. Spectral scaling factors: 35°C (×1.833), 2°C (×1).

1204 to 1224 cm^{-1} due to residual $CHCl_3$ are evident.

In the high wavenumber region, the features of both the 3.52 (Fig. 6B) and the 2.34 (Fig. 7B) μmol m^{-2} C_{18} phases equilibrated in $CHCl_3$ exhibit subtle changes with temperature. The ν_s $(CH_3)/\nu_a$ (CH_2) band shifts from 2895.8 to 2888.2 cm^{-1} for the 3.52 μmol/m^2 C_{18} phase, and from 2894.2 to 2892.7 cm^{-1} for the 2.34 μmol m^{-2} C_{18} phase, in going from 35 to 2°C. However, unlike in the presence of the other mobile phases, the ν_s $(CH_3)/\nu_a$ (CH_2) band from $CHCl_3$ does not appear to become drastically more narrow for this change in temperature, and in fact, the ν_s $(CH_3)/\nu_a$ (CH_2) band due to the 2.34 μmol m^{-2} C_{18} phase actually appears to be broader at 2°C than at 35°C (Fig. 7B). The ν_s (CH_2) band of the bonded C_{18} ligands is also temperature sensitive in $CHCl_3$, but again unlike in the other mobile phase solvents, the band position remains essentially unchanged at about 2851.9 cm^{-1} for both stationary phase bonding densities at either temperature, and the band intensity actually increases in going from 35 to 2°C. Another thing to note in regards to the bonded ligand spectral features obtained from $CHCl_3$, is that the more prominent shoulder due to methylene asymmetric stretching [ν_a (CH_2)] that was observed for the 2.34 μmol m^{-2} C_{18} phase at 35°C in comparison to the 3.52 μmol m^{-2} C_{18} phase features [40], is also observed for this same stationary phase at 2°C (Fig. 7B).

3.4. [I ν_s (CH_3)/I ν_s (CH_2)] as a qualitative measure of alkyl chain conformational ordering

The peak frequencies and the ratio of peak heights of the band at ~2890 cm^{-1} to the band at ~2850 cm^{-1} have been shown to provide information about

alkyl chain conformations [44–46]. The band at ~2850 cm^{-1} has consistently been assigned to methylene symmetric stretching, whereas the band at ~2890 cm^{-1} has been assigned to methylene asymmetric stretching [44–46] and to methyl symmetric stretching [42,43]. This broad band at ~2890 cm^{-1} results from the combination of overlapping features due to both methyl symmetric stretching [ν_s (CH_3)] and methylene asymmetric stretching [ν_a (CH_2)], and thus this band has been referred to several times herein as the ν_s (CH_3)/ν_a (CH_2) band. The present assignment of the ~2890 cm^{-1} band to methyl symmetric stretching is based upon several observations, including that the relative spectral intensity decreases in both the ~2850 and ~2925 cm^{-1} regions but increases in the ~2890 cm^{-1} region when octadecane undergoes a liquid-to-solid phase transition, which is consistent with the dramatic reduction of all modes of methylene stretching upon freezing. Thus, the ratio of peak heights of the band at ~2890 cm^{-1} to the band at ~2850 cm^{-1}, which has been referred to as I_{2890}/I_{2850} [44], [$I_{\approx 2890}/I_{\approx 2850}$] [45], and [$I\ \nu_a$ (CH_2)/$I\ \nu_s$ (CH_2)] [46], is herein denoted [$I\ \nu_s$ (CH_3)/$I\ \nu_s$ (CH_2)].

Table 1 summarizes the [$I\ \nu_s$ (CH_3)/$I\ \nu_s$ (CH_2)] intensity ratios and peak frequencies observed for octadecane, and for the bonded phases exposed to different mobile phase environments, as a function of temperature. Fig. 8 compares the [$I\ \nu_s$ (CH_3)/$I\ \nu_s$ (CH_2)] intensity ratios for octadecane and for both the 3.52 and the 2.34 μmol m^{-2} C_{18} stationary phase ligands exposed to water, as a function of temperature from 45 to 2°C. The intensity ratios for octadecane change from a value of ~0.85 for liquid octadecane to a value of ~1.52 for solid octadecane;

Table 1
[$I\ \nu_s$ (CH_3)/$I\ \nu_s$ (CH_2)] intensity ratios and maximum peak height frequencies (cm^{-1}) of the ν_s (CH_2) and ν_s (CH_3) bands as a function of stationary phase (μmol m^{-2} C_{18}), mobile phase, and temperature

Stationary phase/ mobile phase	[$I\ \nu_s$ (CH_3)/$I\ \nu_s$ (CH_2)] (ν_s (CH_2), ν_s (CH_3))				
	45°C	35°C	25°C	12.5°C	2°C
Octadecane	0.8516 (2853.4, 2891.2)	0.8601 (2853.4, 2889.7)	1.523 (2850.3, 2880.6)	1.516 (2850.3, 2879.1)	1.526 (2850.3, 2879.1)
3.52/H_2O	1.101 (2853.4, 2891.2)	1.108 (2851.9, 2889.7)	1.112 (2851.9, 2886.7)	1.143 (2851.9, 2885.2)	1.177 (2850.3, 2883.7)
2.34/H_2O	1.125 (2853.4, 2892.7)	1.106 (2853.4, 2891.2)	1.109 (2851.9, 2891.2)	1.138 (2851.9, 2886.7)	1.172 (2850.3, 2883.7)
3.52/ACN		1.136 (2853.4, 2889.7)			1.169 (2851.9, 2885.2)
2.34/ACN		1.133 (2853.4, 2892.7)			1.117 (2851.9, 2889.7)
3.52/MeOH		1.152 (2853.4, 2895.8)			1.203 (2851.9, 2883.7)
2.34/MeOH		1.109 (2851.9, 2895.8)			1.153 (2851.9, 2892.7)
3.52/$CHCl_3$		1.050 (2851.9, 2895.8)			1.035 (2851.9, 2888.2)
2.34/$CHCl_3$		1.054 (2851.9, 2894.2)			1.029 (2851.9, 2892.7)

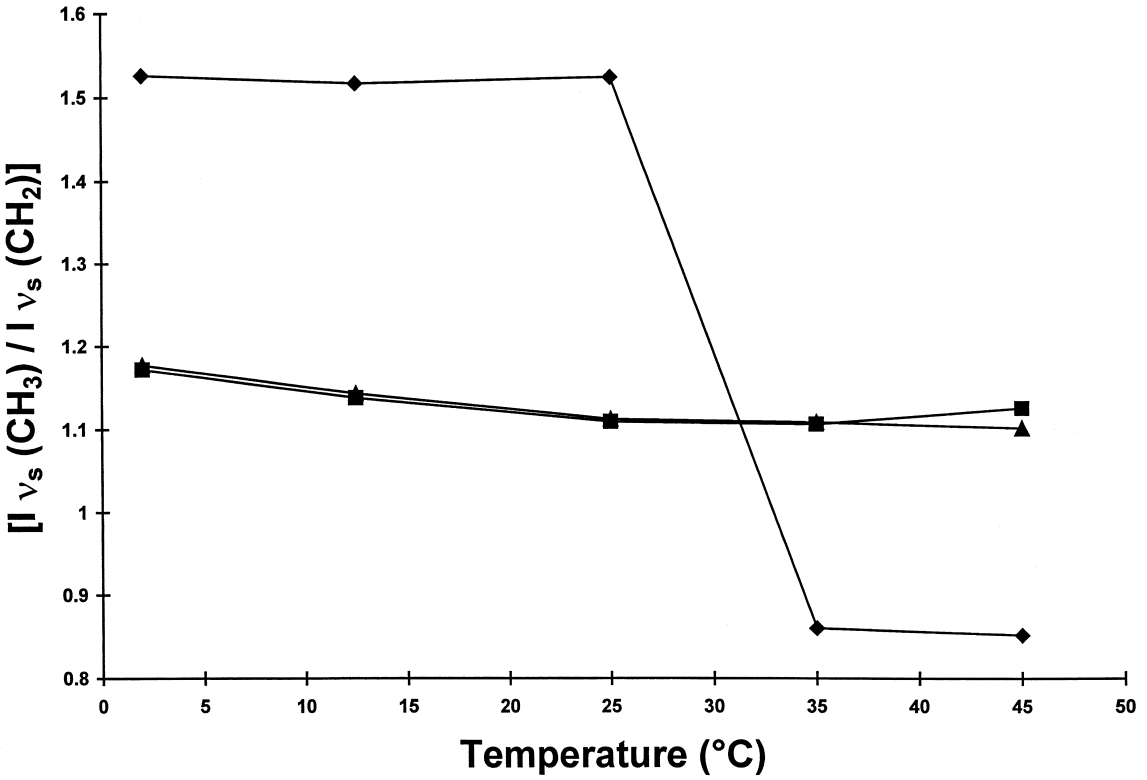

Fig. 8. [I ν_s (CH_3)/I ν_s (CH_2)] intensity ratios for neat octadecane (♦) and for both the 3.52 (▲) and the 2.34 (■) μmol m^{-2} Microporasil C_{18} stationary phase ligands exposed to water, as a function of temperature from 45 to 2°C.

whereas the ratios are generally observed to gradually increase from a value of ~1.11 at 45°C to a value of ~1.17 at 2°C for both stationary phases (Fig. 8). With the exception of the value for the 2.34 μmol m^{-2} C_{18} stationary phase at 45°C, the ratios at each temperature are very close to one another for both stationary phases exposed to an aqueous environment. The differences observed at 45°C for the stationary phases is again largely due to spectral background differences which have slightly reduced the relative intensity of the ν_s (CH_2) band for the 2.34 μmol m^{-2} C_{18} stationary phase. The value of the intensity ratio obtained for a sample can be compared to that of a standard, in this case octadecane, to estimate the degree of alkyl chain order [44–46]. Thus a highly ordered system would have an intensity ratio value closer to that of solid octadecane (~1.52); whereas a disordered system intensity ratio value would be closer to that of liquid octadecane (~0.85). Therefore, based upon intensity ratio values alone, the aqueous exposed bonded phases would be considered to have alkyl chain conformations more closely resembling liquid than solid octadecane, although the ratios obtained at 2°C for the bonded phases (~1.17) fall nearly in the middle of the values obtained for liquid and solid octadecane. Certainly, the general trend of gradually increasing bonded ligand order with decreasing temperature, as previously discussed and observed throughout both spectral regions examined, is again supported by the intensity ratios determined for the aqueous exposed bonded phases (Fig. 8).

Several different trends are obtained however, when examining the rather limited data obtained for the bonded phases exposed to other mobile phase environments (Fig. 9). The [I ν_s (CH_3)/I ν_s (CH_2)] intensity ratios for both the 3.52 and the 2.34 μmol m^{-2} C_{18} stationary phase ligands, exposed to the different mobile phase environments, at 35 and 2°C are shown in Fig. 9. For comparison, the intensity

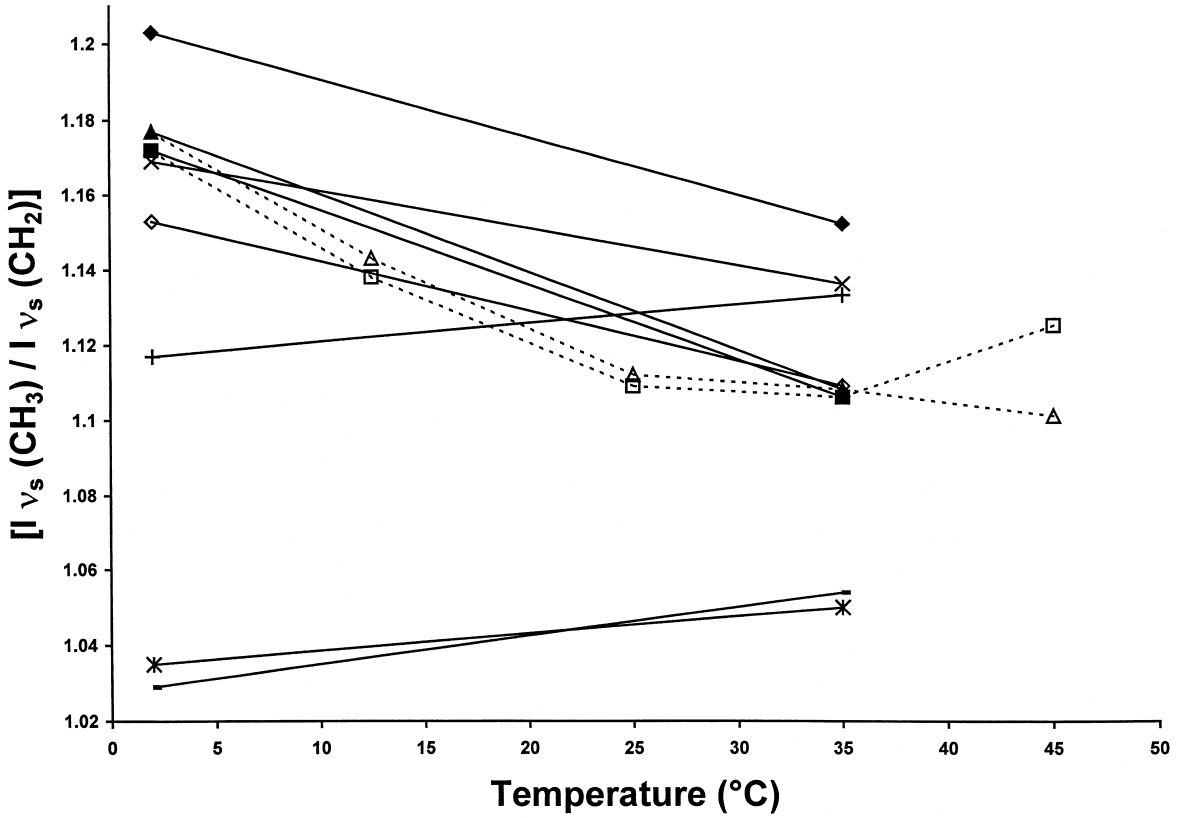

Fig. 9. [I ν_s (CH_3)/I ν_s (CH_2)] intensity ratios for the 3.52 μmol m^{-2} Microporasil C_{18} stationary phase ligands exposed to acetonitrile (×), chloroform (*), methanol (♦), and water (▲), and for the 2.34 μmol m^{-2} Microporasil C_{18} stationary phase ligands exposed to acetonitrile (+), chloroform (−), methanol (◇), and water (■) at 35 and 2°C. For comparison, the intensity ratios obtained over the entire temperature range investigated (45 to 2°C) for both the 3.52 (△) and the 2.34 (□) μmol m^{-2} Microporasil C_{18} stationary phase ligands exposed to water (dashed lines) are also shown.

ratios obtained over the entire temperature range investigated (45 to 2°C) for both the 3.52 and the 2.34 μmol m^{-2} C_{18} stationary phases exposed to water (dashed lines) are also shown in Fig. 9. Examination of the intensity ratios obtained at 35°C indicates that, in comparison to water, both methanol (especially for the 3.52 μmol m^{-2} C_{18} phase) and to a lesser extent acetonitrile induce more ordering of the bonded phase ligands; whereas chloroform induces less ligand ordering. The ratio for the 2.34 μmol m^{-2} C_{18} stationary phase ligands exposed to methanol at 35°C is comparable to the ratios obtained for both the stationary phases exposed to water. Decreasing the temperature from 35 to 2°C increases the ligand ordering for the stationary phases exposed to water and methanol, and for the 3.52 μmol m^{-2} C_{18} stationary phase exposed to acetonitrile. The relative mobile phase induced ordering in going from 35 to 2°C, as measured by the relative change in ratio values at these temperatures (Δ, where Δ=ratio at 2°C−ratio at 35°C), is slightly higher for water (Δ=0.069 and 0.066 for the 3.52 and 2.34 μmol m^{-2} C_{18} stationary phases, respectively) than for methanol (Δ=0.051 and 0.044 for the 3.52 and 2.34 μmol m^{-2} C_{18} stationary phases, respectively), and considerably less for acetonitrile in the case of the 3.52 μmol m^{-2} C_{18} stationary phase (Δ=0.033). The relative temperature induced ordering as indicated by the intensity ratios is such that at 2°C, both phases exposed to water are actually more ordered than either the 2.34 μmol m^{-2} C_{18} stationary phase exposed to methanol or both phases

exposed to acetonitrile. Also, decreasing the temperature actually reduces the ratios for the 2.34 μmol m^{-2} C_{18} stationary phase exposed to acetonitrile ($\Delta = -0.016$) and both phases exposed to chloroform ($\Delta = -0.015$ and -0.025 for the 3.52 and 2.34 μmol m^{-2} C_{18} stationary phases, respectively).

The results obtained based solely on comparisons of the [$I\ \nu_s\ (CH_3)/I\ \nu_s\ (CH_2)$] intensity ratios alone have raised several questions that warrant future investigation. As noted previously [40], the use of deuterated solvents and/or stationary phases would minimize the spectral overlap between stationary phase and mobile phase features and allow more complete subtraction of acetonitrile and methanol features from the features due to the bonded phase ligands. A priori, one would not necessarily expect water to induce more ordering of the bonded phase ligands than the acetonitrile and methanol mobile phases, even on a relative basis as Δ indicates, with decreasing temperature, although 2°C is approaching the freezing point of water.

The decreased ordering of the 2.34 μmol m^{-2} C_{18} stationary phase ligands exposed to acetonitrile at 2°C, as indicated by the intensity ratios, contradicts the changes observed for the bonded ligand spectral features of this phase (not shown) at 35 and 2°C. Although subtraction of mobile phase features was incomplete for this phase, increases in $\nu_a\ (C–C)_T$ and $\nu_s\ (C–C)_T$, the slight increase and narrowing of the $\tau\ (CH_2)$ band, narrowing of the $\delta_a\ (CH_3)/\delta_{sci}\ (CH_2)$ band, shifting of both the $\nu_s\ (CH_2)$ and $\nu_s\ (CH_3)/\nu_a\ (CH_2)$ bands to lower energy, and the slight narrowing of the $\nu_s\ (CH_3)/\nu_a\ (CH_2)$ band were all observed upon decreasing the temperature. These multiple spectral changes indicate that increased ordering of the bonded phase ligands with decreased temperature also occurs for the 2.34 μmol m^{-2} C_{18} stationary phase ligands exposed to acetonitrile, in contrast to the decreased order indicated by the [$I\ \nu_s\ (CH_3)/I\ \nu_s\ (CH_2)$] ratios.

As previously discussed [40], the stationary phase ligands were not observed to undergo a reorganization from a collapsed conformation in a polar aqueous environment to an extended conformation in the decreasingly polar acetonitrile, methanol, and chloroform environments, due to the lack of significant spectral changes in the C–C stretching features of the bonded ligands with mobile phase changes. The most dramatic changes observed, however, resulted in increased methylene stretching when the stationary phase ligands were exposed to chloroform. The changes observed due to chloroform were presumed to provide a slightly more ordered ligand configuration according to the present theories of alkyl chain conformations being susceptible to solvent polarity differences. The exact ligand conformations in different mobile phase environments is still elusive, and it may be quite possible that, as indicated by the [$I\ \nu_s\ (CH_3)/I\ \nu_s\ (CH_2)$] ratio values, chloroform is actually inducing more dissorder into the bonded phase ligand system than the other mobile phases. However, conclusions based solely upon the [$I\ \nu_s\ (CH_3)/I\ \nu_s\ (CH_2)$] ratio values are questionable with regards to the effect of chloroform on stationary phase ligand organization. The ratio values indicate that chloroform induces more ligand disorder with decreasing temperature; whereas the observed spectral changes with temperature, particularly for the 3.52 μmol m^{-2} C_{18} stationary phase, support the conclusion that increased ligand ordering occurs with decreased temperature even in a chloroform mobile phase environment. For instance, in the case of the 3.52 μmol m^{-2} C_{18} stationary phase exposed to chloroform (Fig. 6), increases in $\nu_a\ (C–C)_T$ and $\nu_s\ (C–C)_T$, the slight increase and narrowing of the $\tau\ (CH_2)$ band, narrowing of the $\delta_a\ (CH_3)/\delta_{sci}\ (CH_2)$ band (more readily apparent upon superimposition; not shown), and the shifting of the $\nu_s\ (CH_3)/\nu_a\ (CH_2)$ band to lower energy are all observed upon decreasing the temperature. Definitely, a complete understanding of the origins of the ligand spectral differences observed upon exposure to chloroform and other solvents, as well as the changes in ligand orientations which these spectral differences relate to, will provide new insights into the molecular interactions that occur during solute retention in reversed-phase separations.

4. Summary and conclusions

Raman spectroscopic characterization of the temperature-dependent behavior of bonded C_{18} ligands under solvated conditions reveals that the conformations of the ligands are susceptible to changes in temperature. The bonded ligands do not exhibit the

same ''phase transition'' behavior as neat octadecane, in which the octadecane melts at a discrete temperature (28–30°C). Rather, the spectral features of the C_{18} ligands, which more closely resemble those of liquid than solid octadecane, are observed to gradually and continually vary with changes in temperature over the range investigated (2–45°C). The spectral features of the bonded ligands become more narrow with decreasing temperature. The narrowing of the spectral features, and associated spectral shifts, is indicative of the bonded ligands becoming increasingly more ordered as the temperature is reduced. This temperature-induced ordering is verified by the spectral changes observed for neat octadecane over the temperature range investigated.

The temperature-induced ordering of the bonded phase ligands was observed for both the 2.34 and the 3.52 μmol m^{-2} C_{18} Microporasil stationary phases exposed to water and chloroform, although the changes in chloroform were much more subtle. It should be noted that the nonlinear van't Hoff behavior that has been observed and attributed to possible phase transitions, were typically only observed for high bonding density monomeric phases (>3.5 μmol m^{-2}), whereas the present Raman spectroscopic studies indicate that similar temperature dependencies are observed for both the stationary phases used in this study. Even with the difficulties of subtracting solvent features from the bonded ligand features in acetonitrile and methanol mobile phase environments, temperature-induced ligand ordering similar to that found in water was also observed in both acetonitrile and methanol.

Acknowledgements

The technical expertise of Mr. Keith Collins for assistance in the design and manufacture of the Raman/LC columns and the Raman liquid/solid cells employed in this study is gratefully acknowledged. The synthesis of the Microporasil C_{18} stationary phases by Ms. Jessica Wysocki is also gratefully acknowledged. The authors are grateful for support of this work by NIH GM-48561 and JGD is grateful to Merck Research Laboratories for continued support of our work.

References

[1] L.C. Sander, S.A. Wise, Anal. Chem. 61 (1989) 1749.
[2] K.B. Sentell, A.N. Henderson, Anal. Chim. Acta 246 (1991) 139.
[3] M. Pursch, S. Strohschein, H. Händel, K. Albert, Anal. Chem. 68 (1996) 386.
[4] H. Chen, C. Horváth, J. Chromatogr. A 705 (1995) 3.
[5] P.L. Zhu, L.R. Snyder, J.W. Dolan, N.M. Djordjevic, D.W. Hill, L.C. Sander, J. Chromatogr. A 756 (1996) 21.
[6] P.L. Zhu, J.W. Dolan, L.R. Snyder, J. Chromatogr. A 756 (1996) 41.
[7] P.L. Zhu, J.W. Dolan, L.W. Snyder, D.W. Hill, L. Van Heukelem, T.J. Waeghr, J. Chromatogr. A 756 (1996) 51.
[8] P.L. Zhu, J.W. Dolan, L.R. Snyder, N.M. Djordjevic, D.W. Hill, J.-T. Lin, J. Chromatogr. A 756 (1996) 63.
[9] L.C. Sander, L.R. Field, Anal. Chem. 52 (1980) 2009.
[10] R.K. Gilpin, J.A. Squires, J. Chromatogr. Sci. 19 (1981) 195.
[11] A. Nahum, C. Horvath, J. Chromatogr. 203 (1981) 53.
[12] E. Grushka, H. Colin, G. Guiochon, J. Chromatogr. 248 (1982) 325.
[13] K. Jinno, T. Nagoshi, N. Tanaka, M. Okamoto, J.C. Fetzer, W.R. Biggs, J. Chromatogr. 436 (1988) 1.
[14] A. Tchapla, S. Heron, H. Colin, G. Guiochon, Anal. Chem. 60 (1988) 1443.
[15] H.J. Issaq, M. Jaroniec, J. Liq. Chromatogr. 12 (1989) 2067.
[16] F.M. Yamamoto, S. Rokushika, H. Hatano, J. Chromatogr. Sci. 27 (1989) 704.
[17] L.A. Cole, J.G. Dorsey, Anal. Chem. 64 (1992) 1317.
[18] L.A. Cole, J.G. Dorsey, K.A. Dill, Anal. Chem. 64 (1992) 1324.
[19] R.K. Gilpin, M.E. Gangoda, A.E. Krishen, J. Chromatogr. Sci. 20 (1982) 345.
[20] D. Morel, J. Serpinet, J. Chromatogr. 248 (1982) 231.
[21] W.E. Hammers, P.B.A. Verschoor, J. Chromatogr. 282 (1983) 41.
[22] J.W. Carr, J.M. Harris, J. Chromatogr. 481 (1989) 135.
[23] D. Morel, J. Serpinet, J. Chromatogr. 200 (1980) 95.
[24] D. Morel, J. Serpinet, J. Chromatogr. 214 (1981) 202.
[25] Z. Kessaissia, E. Papirer, J.-B. Donnet, J. Colloid Interface Sci. 79 (1981) 257.
[26] D. Morel, J. Serpinet, G. Untz, Chromatographia 18 (1984) 611.
[27] P. Claudy, J.M. Letoffé, C. Gaget, D. Morel, J. Serpinet, J. Chromatogr. 329 (1985) 331.
[28] D. Morel, K. Tabar, J. Serpinet, P. Claudy, J.M. Letoffe, J. Chromatogr. 395 (1987) 73.
[29] S.S. Yang, R.K. Gilpin, J. Chromatogr. 449 (1988) 115.
[30] J.F. Wheeler, T.L. Beck, S.J. Klatte, L.A. Cole, J.G. Dorsey, J. Chromatogr. A 656 (1993) 317.
[31] F. Riedo, M. Czencz, O. Liardon, E. Kováts, Helv. Chim. Acta 61 (1978) 1912.
[32] J.C. van Miltenburg, W.E. Hammers, J. Chromatogr. 268 (1983) 147.
[33] S.J. Hansen, J.B. Callis, J. Chromatogr. Sci. 21 (1983) 560.
[34] K. Jinno, T. Ibuki, N. Tanaka, M. Okamoto, J.C. Fetzer, W.R. Biggs, P.R. Griffiths, J.M. Olinger, J. Chromatogr. 461 (1989) 209.

[35] L.C. Sander, J.B. Callis, L.R. Field, Anal. Chem. 55 (1983) 1068.
[36] K.B. Sentell, J. Chromatogr. A 656 (1993) 231.
[37] K.B. Sentell, D.M. Bliesner, S.T. Shearer, in: J.J. Pesek, I.E. Leigh (Eds.), Chemically Modified Surfaces, Royal Society of Chemistry, Cambridge, 1994, p. 190.
[38] J.P. Beaufils, M.C. Hennion, R. Rosset, Anal. Chem. 57 (1985) 2593.
[39] J. Wawryszczuk, M. Lewandowski, W. Górniak, J. Goworek, T. Goworek, Chromatographia 25 (1988) 721.
[40] C.A. Doyle, T.J. Vickers, C.K. Mann, J.G. Dorsey, J. Chromatogr. A, (the first of two papers).
[41] C.A. Doyle, T.J. Vickers, C.K. Mann, J.G. Dorsey, J. Chromatogr. A 779 (1997) 91.
[42] D. Lin-Vien, N.B. Colthup, W.G. Fateley, J.G. Grasselli, The Handbook of Infrared and Raman Characteristic Frequencies of Organic Molecules, Academic Press, New York, 1991.
[43] R.M. Silverstein, G.C. Bassler, T.C. Morrill, Spectrometric Identification of Organic Compounds, 5th ed, John Wiley and Sons, New York, 1991.
[44] B.P. Gaber, W.L. Peticolas, Biochim. Biophys. Acta 465 (1977) 260.
[45] D.F.H. Wallach, S.P. Verma, J. Fookson, Biochim. Biophys. Acta 559 (1979) 153.
[46] M. Ho, M. Cai, J.E. Pemberton, Anal. Chem. 69 (1997) 2613.